Solution Structural Studies of the Saccharomyces cerevisiae TATA Binding Protein (TBP) †

3 AUTHORS, INCLUDING:

Sergei Khrapunov
Albert Einstein College of Medicine
85 PUBLICATIONS **352** CITATIONS

SEE PROFILE

Nina Pastor
Universidad Autónoma del Estado de Morelos
48 PUBLICATIONS **491** CITATIONS

SEE PROFILE

Solution Structural Studies of the *Saccharomyces cerevisiae* TATA Binding Protein (TBP)[†]

Sergei Khrapunov,*,[‡] Nina Pastor,[§] and Michael Brenowitz*,[‡]

Department of Biochemistry, Albert Einstein College of Medicine, 1300 Morris Park Avenue, Bronx, New York 10461, and Facultad de Ciencias, UAEM, Av. Universidad 1001, Col. Chamilpa, 62210 Cuernavaca, Morelos, Mexico

ABSTRACT: The intrinsic fluorescence of the six tyrosines located within the C-terminal domain of the *Saccharomyces cerevisiae* TATA binding protein (TBP) and the single tryptophan located in the N-terminal domain has been used to separately probe the structural changes associated with each domain upon DNA binding or oligomerization of the protein. The unusually short-wavelength maximum of TBP fluorescence is shown to reflect the unusually high quantum yield of the tyrosine residues in TBP and not to result from unusual tryptophan fluorescence. The anisotropy of the C-terminal tyrosines is very high in monomeric, octameric, and DNA-complexed TBP and comparable to that observed in much larger proteins. The tyrosines have low accessibility to an external fluorescence quencher. The anisotropy of the single tryptophan located within the N-terminal domain of TBP is much lower than that of the tyrosines and is accessible to an external fluorescence quencher. Tyrosine, but not tryptophan, fluorescence is quenched upon TBP−DNA complex formation. Only the tryptophan fluorescence is shifted to longer wavelengths in the protein−DNA complex. In addition, the accessibility of the tryptophan residue to the external quencher and the internal motion of the tryptophan residue increase upon DNA binding by TBP. These results show the following: (i) The structure of the C-terminal domain structure is unchanged upon TBP oligomerization, in contrast to the N-terminal domain [Daugherty, M. A., Brenowitz, M., and Fried, M. G. (2000) *Biochemistry 39*, 4869−4880]. (ii) The environment of the tyrosine residues within the C-terminal domain of TBP is structurally rigid and unaffected by oligomerization or DNA binding. (iii) The C-terminal domain of TBP is uniformly in close proximity to bound DNA. (iv) While the N-terminal domain unfolds upon DNA binding by TBP, its increased correlation time shows that the overall structure of the protein is more rigid when complexed to DNA. A model that reconciles these results is proposed.

The formation of a transcription preinitiation complex (PIC)[1] involves binding of RNA polymerase II to a promoter facilitated by the assembly of an ensemble of RNA polymerase-specific transcription factors. The binding of the complex TFIID to a specific sequence, a TATA box, initiates assembly of PIC (*1*, *2*). The TATA binding protein (TBP) recognizes and binds to the TATA box sequence and is thus central to PIC assembly. Crystallographic studies have shown that TBP binds to and unwinds the minor groove of the DNA, exposing a broad flat surface to the protein; the DNA is dramatically bent, stabilized by the intercalation of phenylalanine residues at DNA kinks present at either end of the complex (*3−8*). Solution studies of TBP−DNA complexes by time-resolved fluorescence resonance energy transfer (FRET) reveal dramatic differences in both the end-to-end

distances and the distributions of distances for TBP-bound DNA bearing different TATA sequences (*9*) that are highly sensitive to the osmolyte concentration in some cases (*10*).

Saccharomyces cerevisiae TBP is a single polypeptide of 240 residues consisting of a highly conserved C-terminal domain of 180 residues (∼80% sequence identity among all eukaryotic species) and an N-terminal domain of 60 residues that is poorly conserved and variable in length (18−173 residues). In contrast to the large DNA conformation changes observed upon TBP binding, comparison of the crystal structures of free TBP (*11−14*) with the cocrystal structures indicates that the protein structure changes little upon DNA binding. Only a small reorientation of the two subdomains of the DNA binding domain of TBP relative to the 2-fold axis is observed. There is no change in secondary structure. However, the above referenced crystal structures are either of the C-terminal core of TBP (for the yeast and human proteins) or of *Arabidopsis thaliana* TBP which has a short (18 residue) unstructured N-terminal domain. Thus, only limited information is available about the structural features of the N-terminal domain of TBP and its relationship to the C-terminal domain.

The intrinsic fluorescence of tyrosine and tryptophan residues has long been an insightful probe of the microenvironment in proteins because of the nonradiative decay

* To whom correspondence should be addressed (S.K.: khraps@ aecom.yu.edu; M.B.: brenowit@aecom.yu.edu).

[‡] Albert Einstein College of Medicine.

[§] Facultad de Ciencias, UAEM.

[1] Abbreviations: PIC, preinitiation complex; TBP, TATA binding protein; HSA, human serum albumin; N-Tyr, *N*-acetyl-L-tyrosine ethyl ester; N-Trp, *N*-acetyl-L-tryptophan ethyl ester; FRET, fluorescence resonance energy transfer; AdMLP, adenovirus major late promoter.

pathways available to the indole and phenol chromophores (15, 16). A structural peculiarity of TBP permits the effective application of intrinsic fluorescence to its study. Six tyrosines and no tryptophan are found within the C-terminal domain of *S. cerevisiae* TBP. A single tryptophan and no tyrosines are found within N-terminal domain of the protein. Thus, these fluorophores can be used to selectively probe the structure of each domain.

Although *S. cerevisiae* TBP binds specific sequences of DNA as a monomer both in the crystals and in solution, it oligomerizes in solution to octamers under the experimental conditions of the present study (17). Tryptophan fluorescence has been effectively used to study this protein as a function of oligomerization (18, 19). Tryptophan's spectrum undergoes a shift to longer wavelengths when TBP binds to DNA; it was suggested that the unusually short-wavelength maximum of the TBP fluorescence spectrum comes from a low polar environment in the N-terminal domain (18). The anisotropy of the tryptophan fluorescence was shown to be minimally dependent on TBP oligomerization. Rather, it reflects the relaxation time of the N-terminal domain itself within the protein (19).

The present studies compare the intrinsic tyrosine and tryptophan fluorescence of *S. cerevisiae* TBP in order to separately probe the structural changes of the C- and N-terminal domains as a function of protein ligation and oligomerization. Selective excitation has been used to separate the contributions of tyrosine and tryptophan residues to the TBP fluorescence spectra. Several features of TBP fluorescence are reinterpreted in light of these new data. Insight into the structural correlates of the fluorescence data is obtained by an analysis of molecular dynamics simulations of free and DNA-bound TBP.

EXPERIMENTAL PROCEDURES

Protein, DNA, and Other Reagents. TATA binding protein from *S. cerevisiae* was expressed in *Escherichia coli* and purified as previously described (20, 21). An extinction coefficient of $13.4 \times 10^3 \ M^{-1} \ cm^{-1}$ was used to calculate the TBP concentration. Human serum albumin (HSA, 99%, HPCE, Fluka) and *N*-acetyl-L-tyrosine (N-Tyr) and *N*-acetyl-L-tryptophan (N-Trp) ethyl esters (Sigma) were used without additional purification. Labeled and unlabeled DNA oligonucleotides were obtained from TriLink Biotechnologies, Inc. The concentration of oligonucleotides was determined using extinction coefficients calculated from the known base pair composition, correcting for the absorbance of fluorescein and TAMRA at 260 nm for concentration determinations of the labeled oligonucleotides.

The activity of the protein was measured using fluorescence resonance energy transfer (FRET) of a 14 bp oligonucleotide bearing the adenovirus major late promoter (AdMLP) sequence TATAAAAG and double labeled with fluorescein and TAMRA (21, 22). In the present study, separately labeled top and bottom strands were end-annealed to yield the duplex:

Fluorescein - CGCTATAAAAGGGC - 3'
3' - GCGATATTTTCCCG - TAMRA
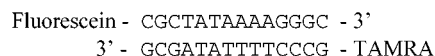
Annealing titrations of the complement were conducted to ensure that the entire DNA present in studies utilizing

DNA was duplex. An unlabeled oligonucleotide of the same sequence was used in the intrinsic fluorescence studies of the TBP−DNA complex.

Fluorescence Spectroscopy. All experiments were performed in buffer containing 25 mM Tris, 100 mM KCl, 5 mM MgCl$_2$, 1 mM CaCl$_2$, at pH 7.5 and 22 °C. Fluorescence measurements were made using a Fluoromax-3 spectrofluorometer (Jobin Yvon Inc., USA). All spectra were corrected for the spectral sensitivity of the instrument. Measurements of the spectra and intensities of fluorescence were performed at the "magic angle" (corresponding to the angle of 55° between the vectors of polarization of the excitation and emission light) to minimize the error due to fluorescence polarization changes (16). The intensity of water's Raman scattering band was used as the internal standard of fluorometer sensitivity. Anisotropy was calculated by

$$A_\lambda = \frac{I_v - GI_h}{I_v - 2GI_h} \tag{1}$$

where A_λ is the fluorescence anisotropy measured at a certain combination of the excitation and emission wavelengths using the vertical position of the excitation polarizer, I_v and I_h are the fluorescence intensities measured at the vertical and horizontal positions of the emission polarizer, and G is the instrumental factor accounting for the bias of the detection system for vertically versus horizontally polarized light.

The absorbance of TBP at 280 nm was not higher than 0.08 at the highest concentrations measured. However, the absorbance of DNA at 275 nm, and less so at 295 nm, must be corrected for in the studies of TBP−DNA complex formation at 6 μM TBP and 12−18 μM 14 bp duplex. To minimize the inner filter effect in these experiments, cuvettes with an optical pathway 3 mm were used, and the inner filter correction (16):

$$F_{corr} = F_{obs} \times 10^{(D_\lambda/2)} \tag{2}$$

was applied for calculations (the spectra are shown without correction), where F_{corr} and F_{obs} are the corrected and observed fluorescence intensities, respectively, and D_λ is the absorbance at the excitation wavelength.

Fluorescence Quenching. Acrylamide was used as a dynamic fluorescence quencher due to its lack of electric charge. Quenching was analyzed by the Stern−Volmer equation (16, 23):

$$\frac{F_0}{F} = \frac{\tau_0}{\tau} = 1 + K_{sv}*[Q] \tag{3}$$

where $F_0(\tau_0)$ and $F(\tau)$ are the fluorescence intensities (lifetimes) of the protein in the absence or presence of the quencher Q, respectively. K_{sv} is the Stern−Volmer (dynamic collision) quenching constant. Anisotropy data were analyzed in terms of the Perrin equation (24):

$$\frac{1}{A} = \frac{1}{A_0} + \frac{\tau}{A_0*\theta} \tag{4}$$

where A is the fluorescence anisotropy, A_0 is the fluorescence anisotropy in the absence of molecular motion, τ is the fluorescence lifetime, and θ is the rotational correlation time.

To determine the limiting anisotropy A_0, $\tau \equiv \tau_{rel} = (\tau/\tau_0) = (F/F_0)$ and $\theta \equiv \theta_{rel} = (\theta/\theta_0)$, the relative changes in the lifetime and the correlation time, respectively, were used. Thus, the limiting anisotropy A_0 is obtained from a plot of $(1/A)$ versus (F/F_0).

When $A \ll A_0$ and $\tau \approx \Theta$, eq 4 can be used for calculation of Θ_{rel}, the relative change in the correlation time of the protein in two structural stages. Let A_{01}, τ_1, and Θ_1 to be the limiting anisotropy, the lifetime, and the correlation time for free TBP while A_{02}, τ_2, and Θ_2 are the same parameters for TBP within the TBP−DNA complex. Combining eq 4 and $(\tau_2/\tau_1) = (F_2/F_1)$ yields

$$\Theta_{rel21} = \frac{\theta_2}{\theta_1} = \frac{(A_{01} - A_1)^* A_2}{(A_{02} - A_2)^* A_1} {}^* \frac{F_2}{F_1} \tag{5}$$

relating the change in the correlation time (Θ_{rel21}) between TBP free and bound to DNA or between TBP monomers and octamers.

Molecular Dynamics Simulations. Simulations were carried out on the C-terminal domain of TBP, both free and in complex with DNA as described previously (*25*). All of the simulations included explicit water molecules (TIP3) and were run with the CHARMM22 all-atom parameter set (*26, 27*). SHAKE was used for all bonds to hydrogen atoms, and the simulations were propagated with a time step of 1.5 fs, for a total duration of 2 ns of production time. Snapshots of the simulations were saved every 50 steps for analysis.

The simulations of the free C-terminal domain of TBP were started from the monomer with the smallest *B*-factors in the crystal structures 1TBP [*S. cerevisiae* (*12*)] and 1VOK [*Arabidopsis thaliana* (*13*)]. As there is no structure for free human TBP, the structure in 1CDW (*7*) was used as a starting point (after deletion of all DNA atoms) because of its higher resolution. The first protein residue present in the simulations is a serine (residue 19 in plant, 61 in yeast, and 155 in human TBP). Hydrogen atoms were added in CHARMM, and their position was energy-refined with 50 steps of minimization. Internal water molecules were included in the simulations (two for 1VOK, and one each for 1TBP and 1CDW). Sufficient water was added to fill a hexagonal prism cell (87 Å in length × 30 Å by side, ∼6000 water molecules). The solvation shell was thoroughly energy-minimized, then heated to 600 K for 10 ps, and equilibrated for 40 ps. The solvation shell was energy-minimized, followed by the energy minimization of the whole system. The whole system was then heated to 300 K in 10 ps, equilibrated for 30 ps with a temperature tolerance of 3 K, and then released for 2 ns of microcanonical dynamics.

Simulations were carried out for six TBP−DNA complexes with the DNA truncated to 12 base pairs in each complex. The yeast, human, and plant TBP C-terminal domains were each simulated with high-affinity and medium-affinity TATA box sequences as follows. Plant TBP was simulated with the dodecamers CTATAAAAGGGC, CTATAATAGGGC, and CTATAAAGAGGGC, corresponding to structures PDT025 (*5*), 1QN6 (*8*), and 1QN5 (*8*), respectively. Yeast TBP was simulated with the dodecamer GTATATAAAACG, after removal of the hairpin in the 1YTB structure (*4*). Human TBP was simulated with the dodecamers GCTATAAAAGGC [from structure 1CDW (*7*)] and CGTATATATACG [from structure 1TGH (*6*)]. The first

residue present in the simulations is the same as described above for the free protein.

The simulation protocol used for the complexes is as described previously (*25*) and above with one difference at the onset of the protocol. Sodium ions were included in the simulations at a ratio of one per phosphate located 3.5 Å from the phosphate atoms along the O−P−O bisector. Once the structures were solvated with ∼6000 TIP3 water molecules, both water and sodium were heated to 600 K during 10 ps and equilibrated for 100 ps, adequate to randomize the counterion positions. This protocol results in stable simulations of the complexes (*25*).

Analysis of the Simulations and of the Crystal Structures. The geometry of the six conserved tyrosine residues was calculated with PROCURVES (*28*) in the version included in the MD Toolchest 1.0 (*29*) for each simulation snapshot and for the available crystal structures of free TBP and TBP−DNA complexes. The data derived from the crystal structures were pooled. The amplitude in motion along χ_1 (the dihedral angle that measures rotation along the bond connecting C_α and C_β) and χ_2 (the dihedral angle that measures rotation along the bond connecting C_β and C_γ) corresponds to the difference of the extreme values of this data set. The amplitude in motion along χ_1 and χ_2 for the simulation data was obtained first for each side chain in each simulation and then averaged over the different simulations.

The solvent accessibility of the tyrosine side chains was calculated with the analytical version of the Lee and Richards algorithm included in CHARMM25 (*30*) using a probe radius of 1.4 Å. To obtain the percentage of exposed surface area, the solvent-accessible area of a single tyrosine side chain was calculated for various χ_1 and χ_2 conformations and averaged, yielding 14.6 Å^2/atom. This value was used to divide the area obtained for each tyrosine and was then multiplied by 100. Solvent accessibility was calculated for all the available crystal structures of free TBP and TBP−DNA complexes, and for every other 1000th snapshot in the simulations. The data for each tyrosine were averaged for each simulation with subsequent averaging of the mean values.

Hydrogen bonds between the tyrosines and the remainder of the protein were calculated for each simulation snapshot with a 2.4 Å cutoff distance between donor and acceptor atoms and no restriction on the angles, using CHARMM25 with the COOR HBOND command.

RESULTS

Proteins display fluorescence only from tryptophan residues when excited at 295 nm due to the lack of absorbance of tyrosine at this wavelength. This property of tryptophan was used to probe differences in the monomeric and octameric oligomers of *S. cerevisiae* TBP; both its spectra and its anisotropy are sensitive to the changes in salt concentration and temperature that mediate oligomerization (*19*). The present study expands upon this work by taking advantage of the localization of the tyrosines and tryptophan of *S. cerevisiae* TBP in the protein's C-terminal and N-terminal domains, respectively, and the fluorescence properties of these residues.

The contributions of both tyrosine and tryptophan residues are monitored by excitation at 275 nm; this characteristic
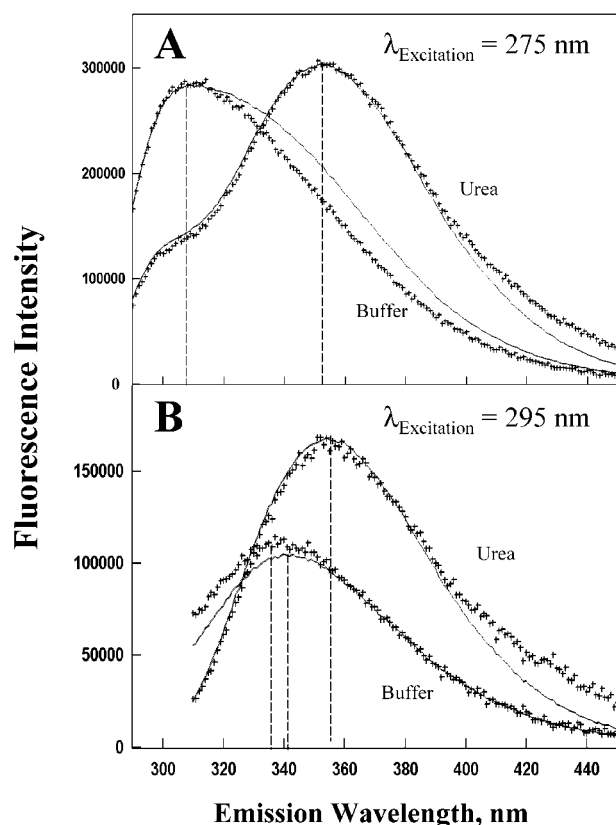
FIGURE 1: Fluorescence emission spectra of *S. cerevisiae* TBP at 1 μM (crossed line) and 6 μM (solid line) concentrations at which the protein is monomeric and octameric, respectively (*17, 19*). Panel A shows the emission spectra obtained using an excitation wavelength of 275 nm. Panel B shows the emission spectra obtained using an excitation wavelength of 295 nm. The fluorescence emission of TBP obtained at 1 μM protein concentration was normalized to the emission obtained at 6 μM at the indicated value of λ_{max}. The solution conditions were 25 mM Tris, 100 mM KCl, 5 mM MgCl$_2$, and 1 mM CaCl$_2$ at pH 7.5 and 22 °C. The curve denoted 'urea' is the buffer described in the previous sentence to which was added 8 M urea.
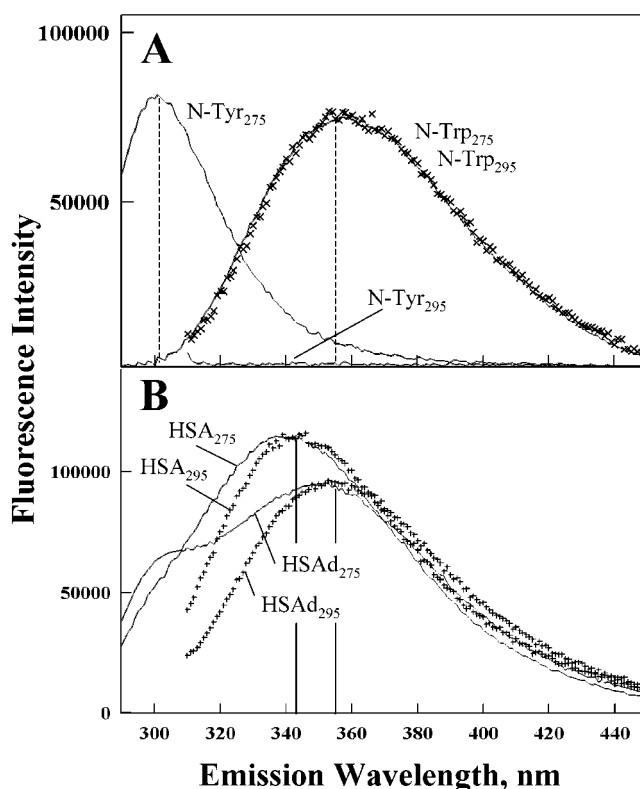

FIGURE 2: Fluorescence emission spectra of model compounds (A) *N*-acetyl-L-tyrosine ethyl ester (N-Tyr) and *N*-acetyl-L-tryptophan ethyl ester (N-Trp) and (B) human serum albumin (HSA) obtained under the conditions of the TBP experiments. The numbers denote the excitation wavelength used upon acquisition of each spectrum. The curves denoted 'd' are the spectra of HSA obtained in the buffer to which was added 8 M urea. The emission spectra obtained using an excitation wavelength of 275 nm are shown by solid lines. The emission spectra of N-Trp and HSA obtained using an excitation wavelength of 295 nm and *normalized to the emission spectra of N-Trp and HSA at the indicated value of λ_{max}* are shown by crossed lines.

has been used to separate the contributions of these two residues to the fluorescence of TBP. The anisotropy of the tyrosine and tryptophan fluorescence and the accessibility of the chromophores to the external quencher probe the dynamics of the two domains of the protein. Energy transfer from tyrosine to tryptophan and from tyrosine to DNA probes the proximity of the C- and N-terminal domains to each other and the C-terminal domain to DNA.

Comparison of Tyrosine/Tryptophan and Tryptophan-Only TBP Fluorescence Emission Spectra. The fluorescence emission maximum, λ_{max}, of *S. cerevisiae* TBP following excitation at 275 nm is ~309 nm for both monomers (1 μM TBP) and octamers (6 μM TBP). The emission spectra of octamers display a shoulder at long wavelengths (Figure 1A). Such a low λ_{max} is rare for tryptophan-containing proteins. When only tryptophan emission is detected by excitation at 295 nm, the emission spectra are typical of tryptophan-containing proteins. Values of λ_{max} of 337 and 341 nm are observed for TBP monomers and octamers, respectively (Figure 1B), that are consistent with previous observations (*19*). The fluorescence emission spectrum of denatured TBP in solution containing 8 M urea is characterized by shifts of λ_{max} to longer wavelengths following excitation at either 275 or 295 nm (Figure 1A,B). The short-wavelength shoulder

evident in the emission spectra of denatured TBP upon excitation at 275 nm is due to the tyrosine fluorescence in the denatured protein (Figure 1A).

Model Compound Analysis. To interpret the unusual aspects of TBP fluorescence, several model systems were analyzed under the present solution conditions. N-Tyr and N-Trp are model compounds reflecting the fluorescence properties of solvent-exposed tyrosine and tryptophan. Human serum albumin (HSA) provides a model for these residues buried inside the protein globule (Figure 2). HSA is similar to *S. cerevisiae* TBP in that it contains a single tryptophan and multiple tyrosine residues. The crystal structure of HSA has been solved, and its single tryptophan is well packed within the interior of the protein surrounded by the tyrosine residues.

The fluorescence spectrum of N-Tyr ($\lambda_{max} \approx 301$ nm) is blue-shifted from that of N-Trp ($\lambda_{max} \approx 358$ nm; Figure 2A). A well-known fluorescence property is that the quantum yield and the shape of a single oscillator's fluorescence spectrum are not dependent upon the excitation wavelength. Confirmation of this property is the perfect match of the emission spectra of N-Trp excited at 275 and 295 nm under these experimental conditions (Figure 2A). Therefore, excitation of TBP at 275 and 295 nm results in identical shape and the quantum yield of the protein's tryptophan fluorescence in

the absence of interaction between the two chromophores. This allows the unique fluorescence properties of the two types of residues to be distinguished.

The λ_{max} for tyrosine fluorescence in proteins is generally comparable to that of free tyrosine, in contrast to the large shifts typically observed for tryptophan (*16*, *31*). The fluorescence spectra of HSA display these characteristics (Figure 2B). Excitation of native HSA at 275 nm yields an emission spectrum that is shifted to the shorter wavelengths compared to that obtained upon excitation at 295 nm. This result demonstrates the contribution of tyrosine residues to emission upon 275 nm excitation. Comparison of the emission spectra of HSA, N-Tyr, and N-Trp shows that the HSA fluorescence at $\lambda < 310$ nm is almost completely due to tyrosine and at $\lambda > 365$ nm is completely due to tryptophan (Figure 2A,B).

Despite the presence of 18 tyrosine residues, the emission spectrum of HSA obtained upon excitation at 295 nm is typical of tryptophan in a nonpolar environment. There is only a slight contribution from tyrosine residues at short wavelengths (Figure 2B). Tyrosine fluorescence is typically quenched in the globular tryptophan-containing proteins mainly due to energy migration from tyrosine to tryptophan (*16*). In 8 M urea, a prominent shoulder in the emission spectrum of HSA appears due to decreased inter-chromophore energy migration and the corresponding increase in the tyrosine fluorescence. Upon denaturation of HSA, λ_{max} for tryptophan and tyrosine fluorescence shifts to that of fully exposed chromophores. Thus, the fluorescence of tyrosines within HSA is characterized by a low quantum yield that rises upon denaturation, and an invariant emission λ_{max} that is similar to that of N-Tyr. In contrast, the fluorescence of the single tryptophan presented in native HSA is characterized by high quantum yield; its emission λ_{max} is shifted to long wavelengths upon protein denaturation, comparable to that of N-Trp. These model compound results allow interpretation of the TBP fluorescence spectra that follow.

Comparison of TBP and Model Compound Emission Spectra. The long-wavelength shoulder in the emission spectrum of octameric TBP corresponds to tryptophan emission. Upon denaturation by 8 M urea, the emission spectra of 1 μM (monomeric) and 6 μM (octameric) TBP converge (Figure 1A,B); λ_{max} is close to that of the solvent-exposed tryptophan (Figure 2A). When the emission spectrum of N-Tyr is first normalized at $\lambda_{max} = 301$ nm to the spectra of monomeric and octameric TBP and then subtracted, the difference spectra correspond closely to the emission spectra of TBP excited directly at 295 nm (compare Figure 3A,B with Figure 1B). Both difference spectra are typical of tryptophan buried within the interior of the protein as can be seen by comparison with the spectra of HSA (Figure 2B). Thus, the unusually short λ_{max} of TBP fluorescence does not result from unusual tryptophan fluorescence, but reflects the unusually high quantum yield of the tyrosine residues within TBP.

The difference spectra λ_{max} shift calculated for monomers relative to octamers (337 to 343 nm; Figure 3) corresponds to the 295 nm excitation λ_{max} (Figure 1B). These results together with the unchanged quantum yield of the tyrosine fluorescence (Table 1) demonstrate that the conformation of the C-terminal domain does not change with TBP oligomerization. In contrast, λ_{max} corresponds to tryptophan within
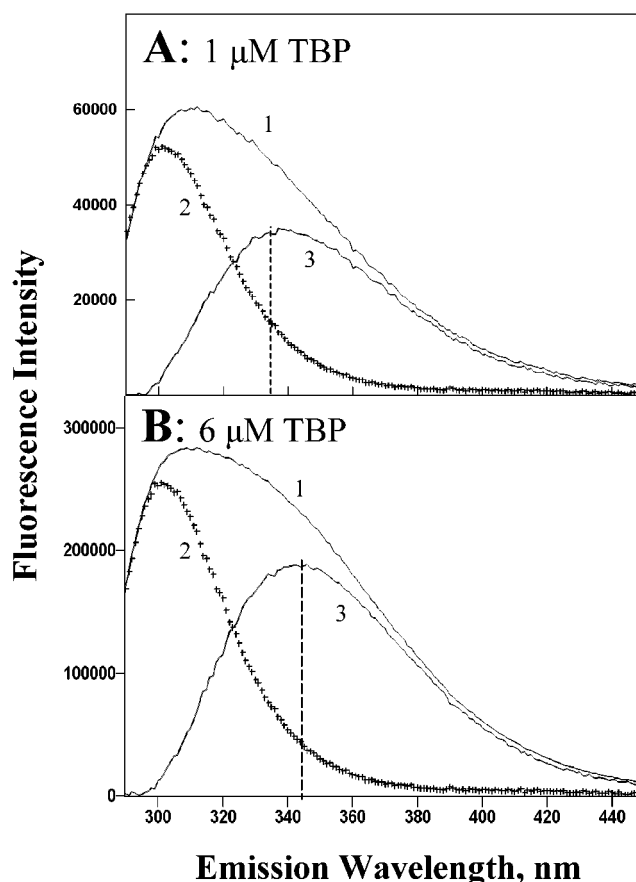

FIGURE 3: Fluorescence emission and difference emission spectra of *S. cerevisiae* TBP at 1 μM (panel A) and 6 μM (panel B) concentrations. The spectrum of N-Tyr (curve 2) was normalized to the short-wavelength part of the TBP spectrum (curve 1). The difference spectrum (curve 3) was obtained by subtraction of spectrum 2 from spectrum 1. The values of difference spectrum λ_{max} of 337 nm (panel A) and 341 nm (panel B) are consistent with the values of λ_{max} obtained upon direct excitation of tryptophan fluorescence of TBP (Figure 1B, Table 1).

Table 1: Comparison of the Fluorescence Properties of Tryptophan and Tyrosine within Monomeric and Octameric TBP and Monomeric TBP Bound to DNA[a]

	theoretical[b]	TBP$_{native}$[c]	TBP$_{denatured}$[d]	TBP$_{DNA}$[e]
R_{Tyr}	1	0.93	1.05	0.93
R_{Trp}	1	1.2	1.03	0.95
$\lambda_{max,Trp(monomer)}$ (nm)	–	337	355	345
$\lambda_{max,Trp(octamer)}$ (nm)	–	341	355	345

[a] The values of R_{Tyr} and R_{Trp} calculated from theory are considered to stem from a 6-fold difference in the concentration of TBP. R_{Tyr} is the ratio of the tyrosine fluorescence of TBP (emission at 306 nm, excitation at 275 nm) while R_{Trp} is the ratio of the tryptophan fluorescence of TBP (emission at 365 nm, excitation at 295 nm) measured at 6 and 1 μM concentration of the protein and normalized by a factor of 6. [b] A value of $R = 1$ assumes no change in a quantum yield of fluorescence of TBP. [c] TBP$_{native}$ – TBP in solution without DNA. [d] TBP$_{denatured}$ – TBP in solution containing 8 M urea. [e] TBP$_{DNA}$ – TBP bound with the DNA.

the N-terminal domain of TBP octamers being in a more polar environment, consistent with published results (*18*, *19*). Thus, the only detectable oligomerization-linked conformational changes are within the N-terminal domain of TBP.

TBP Excitation Spectra. Two factors that can affect the fluorescence intensity of proteins are changes in the absorp-
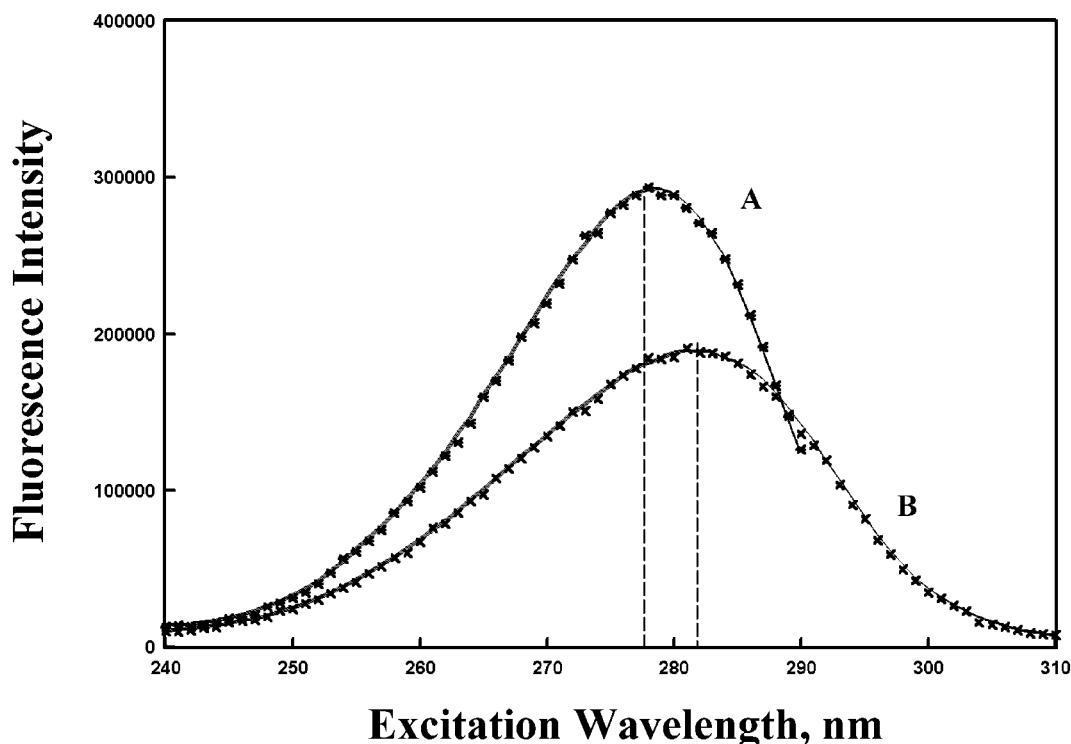
FIGURE 4: Fluorescence excitation spectra of TBP that were obtained for (A) tyrosine, by emission measurement at 306 nm, and (B) tryptophan, by emission measurement 365 nm at protein concentrations of 1 (crossed line) and 6 μM (solid line). The spectra obtained at 1 μM have been normalized to the spectra obtained at 6 μM at their λ_{max} values of 278 nm (A) and 281.5 nm (B), respectively.

tion spectrum and changes in the fluorescence quantum yield. The excitation spectra of TBP obtained when either tyrosine or tryptophan fluorescence emission is monitored are consistent with burial of the tyrosines and a slightly exposed position of the tryptophan (Figure 4). That the excitation spectra of native TBP at 1 and 6 μM match perfectly demonstrates that the emission intensities for monomers and octamers (Table 1) must reflect the difference in the quantum yield of fluorescence of the tyrosine and tryptophan residues. All the values of quantum efficiency in Table 1 are close to unity ($\pm 5-7\%$) with only tryptophan fluorescence in octamers being significantly different. That the quantum yield of tryptophan and the wavelength of λ_{max} of tryptophan fluorescence of TBP are different for octamers as compared with monomers is consistent with only the N-terminal domain changing conformation upon TBP oligomerization.

TBP—TATA Complex. The fluorescence emission spectra of free TBP and TBP bound to a DNA oligonucleotide containing the high-affinity TATA box sequence TATAAAAG are shown in Figure 5. The emission spectra of the TBP—DNA complex match those of monomeric TBP regardless of whether the protein was monomeric (1 μM) or octameric (6 μM) prior to DNA binding. There is no difference in the quantum yield of the tryptophan or tyrosine fluorescence of TBP between TBP—DNA complexes at concentrations of 1 and 6 μM (Table 1). Similarly, the tryptophan quantum yield (Table 1) and anisotropy (Figure 6) in the complex closely match those of the TBP monomer. These results are consistent with the previously observed rapid binding of DNA by *S. cerevisiae* octamers (22) and suggest that only TBP monomer—DNA complexes are present at both proteins concentrations studied.

Both tryptophan and tyrosine fluorescence in proteins have been observed to be quenched upon DNA binding (32).
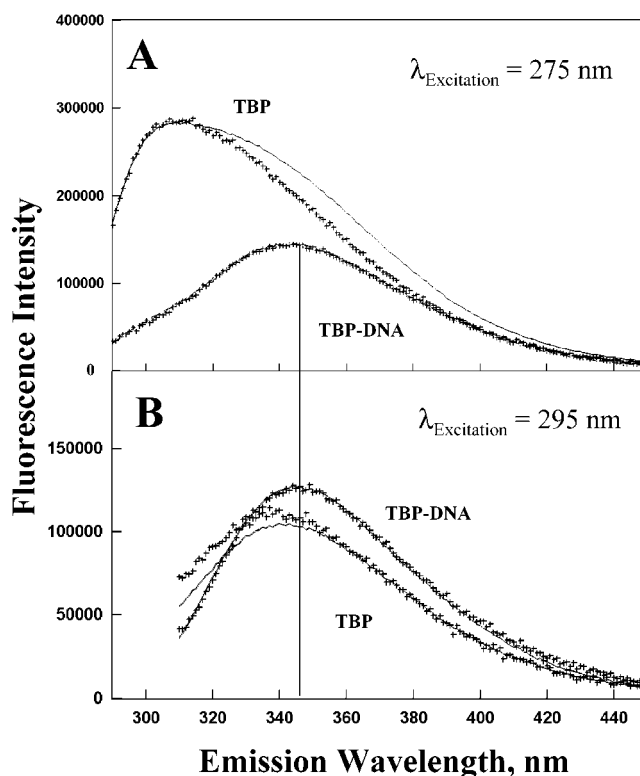

FIGURE 5: Fluorescence emission spectra of TBP free and in complex with DNA at 1 (crossed line) and 6 μM (solid line) concentrations obtained using excitation wavelengths of 275 nm (panel A) and 295 nm (panel B) at a protein:DNA ratio of 1:3. The emission spectrum obtained at 1 μM TBP was normalized to the spectrum obtained at 6 μM at its λ_{max} value of 345 nm.

Resonance energy migration from tyrosines to the base pairs is the main mechanism for tyrosine quenching in protein—nucleic acid complexes due to spectral overlap of the tyrosine
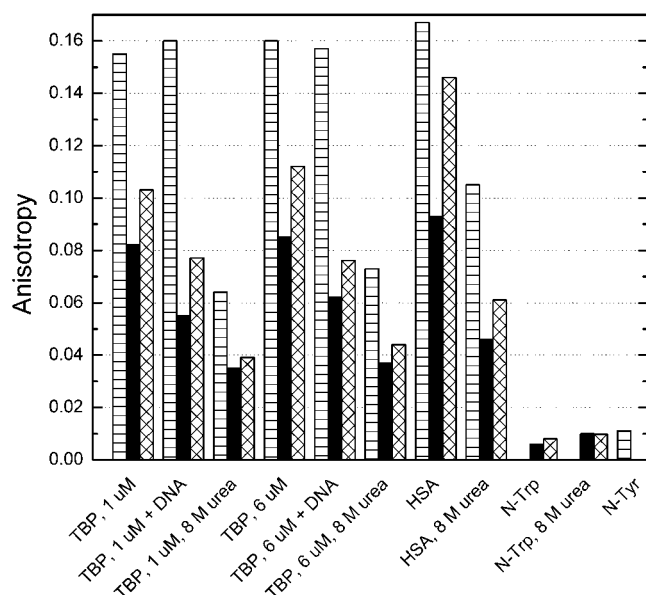
FIGURE 6: Anisotropy of the tyrosine and tryptophan intrinsic fluorescence of TBP compared with model compounds obtained at combinations of excitation and emission wavelengths, respectively, of 275 and 306 nm (hatched bars), 275 and 365 nm (black bars), and 295 and 365 nm (crossed bars). "DNA" denotes the 14 bp oligonucleotide bearing the TATAAAAG sequence at a 1.2 molar ratio to TBP. "+8 M urea" denotes the standard buffer to which 8 M urea was added. The other abbreviations are as defined in the text.

emission spectra and the nucleic acid absorption spectra (*32*). Tyrosine quenching has been used in several studies of tryptophan-free proteins such as histones (*31*). The tyrosine component of the TBP fluorescence spectra (Figures 1 and 3) is equivalently quenched when complexed with DNA at either 1 or 6 μM complex concentrations (Figure 5). This result is consistent with the intimate association of the entire C-terminal domain of TBP to the DNA within the critical distance of 15−20 Å (*33*) required for energy transfer. The tryptophan fluorescence of TBP is increased in the complex (Figure 5). This result is consistent with the tryptophan within the N-terminal domain being outside its critical distance (5−10 Å) (*33*) and not directly participating in the protein−DNA interaction.

Both the quantum yield and the fluorescence spectrum of TBP change upon DNA binding. The change in the emission λ_{max} is 36 and 8 nm upon excitation at 275 and 295 nm, respectively (Figures 5 and 1A,B). These values are different from those measured for TBP denaturation. While the change in the emission λ_{max} obtained upon excitation at 275 nm is mainly due to the contribution of tyrosine fluorescence to the emission spectrum (Figure 5A), the change following excitation at 295 nm reflects a conformation change of the N-terminal domain of TBP upon DNA binding (Figure 5B). The relative quantum yields of the tyrosine and tryptophan fluorescence measured at 1 and 6 μM complex concentrations are identical within experimental error (Table 1).

Fluorescence Anisotropy of the Unliganded and DNA-Bound TBP. The anisotropy of fluorescence of native, denatured, and complexed TBP is summarized in Figure 6 together with that of several model compounds. Tyrosine fluorescence anisotropy is high and the same for monomeric (1 μM) and octameric (6 μM) TBP, suggesting highly restricted tyrosine mobility. Upon TBP denaturation, the

tyrosine fluorescence anisotropy decreases, reflecting a decrease in their relaxation time. The tyrosine anisotropy in native TBP is comparable with that of the much larger protein HSA (Figure 6), suggesting the C-terminal domain of *S. cerevisiae* TBP is exceptionally rigid.

The high anisotropy of tyrosine fluorescence is not changed upon complex formation with DNA. This result demonstrates that the C-terminal domain of TBP does not undergo significant changes in tertiary structure upon DNA binding. The tyrosine side chains are firmly anchored in the C-terminal domain of TBP in both free and DNA-bound protein.

In contrast, the tryptophan fluorescence anisotropy of TBP decreases upon binding to the DNA, as was previously observed (*18*, *19*). However, consideration of the characteristics of tryptophan fluorescence leads to the conclusion that the distance between the C-terminal domain tyrosines and the N-terminal domain tryptophan does not change appreciably upon DNA binding. There are two electronic transitions (^1L_a and ^1L_b) to the first singlet state of tryptophan. Although both transitions are responsible for the absorbance of tryptophan in the range of 240−300 nm, the fluorescence emission of tryptophan is due mainly to the ^1L_a state (*34*). Since the two electronic transitions are oriented perpendicular to each other, tryptophan anisotropy is dependent upon the excitation wavelength, reflecting the relative contributions of the transitions to the absorption spectrum of tryptophan. In addition, energy transfer between the tyrosines and tryptophan decreases the anisotropy of the tryptophan fluorescence in TBP. However, only the latter process (inter-chromophore energy migration) reports changes in the inter-chromophore (tyrosine−tryptophan) distances. Thus, the effect of inter-chromophore energy migration on anisotropy may be isolated by determination of anisotropy ratios at different wavelengths (*35*).

These ratios were determined by monitoring anisotropy emission at 365 nm following excitation at 275 and 295 nm (Figure 6). Both inter- and intramolecular energy migration affect tryptophan anisotropy upon excitation at 275 nm, while only intramolecular energy migration affects it upon excitation at 295 nm. The anisotropy ratios determined for TBP free and complexed with DNA are within experimental error of each other (∼0.76) and lower than that determined for denatured TBP (∼0.87).

An anisotropy change due to intra-chromophore energy migration is independent of protein conformation (*34*). Thus, the decrease in the 275/295 nm anisotropy excitation ratios of tryptophan fluorescence measured for native and denatured TBP must be due to tyrosine to tryptophan energy migration. In contrast, the similarity of these ratios for free and DNA-complexed TBP indicates unchanged energy migration upon ligation of the protein. This result suggests that the average distance between the C-terminal domain tyrosines and the N-terminal domain tryptophan does not change. A limitation to the interpretation of these data is the uncertainty in the Förster radius of the tyrosine−tryptophan pair (*36*) and in the relative orientation of the tyrosine and tryptophan residues.

Fluorescence Quenching. The change in anisotropy, quantum yield, and the λ_{max} of the single tryptophan in the N-terminal domain of TBP indicate flexibility and environmental changes of the chromophore upon binding of the
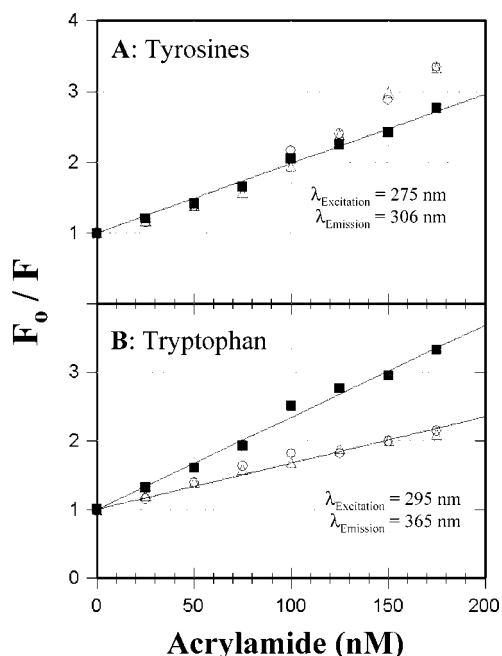
FIGURE 7: Stern−Volmer plots for the quenching by acrylamide of TBP (A) tyrosine fluorescence (excitation at 275 nm and emission at 306 nm) and (B) tryptophan fluorescence (excitation at 295 nm and emission at 365 nm) for TBP at 1 μM (circles), 6 μM (triangles) and for TBP at 6 μM complexed with a 1.2 molar excess of DNA bearing the sequence TATAAAAG (squares).

protein to DNA as compared with the "average" tyrosine in the C-terminal domain. To draw firmer conclusions concerning the mobility of the two domains of TBP, fluorescence was measured as a function of the concentration of a neutral quencher, acrylamide (*23*, *24*).

Quenching of the tyrosine fluorescence is comparable for TBP monomers, octamers, and the TBP−DNA complex (Figure 7A). The Stern−Volmer constants, K_{sv} (eq 3), calculated from these data are comparable to that determined for HSA and much lower than the value determined for free tyrosine in solution (Table 2). These data confirm the low "average" solvent accessibility of the tyrosine residues within the C-terminal domain of TBP independent of oligomerization or ligation. Limitations to the quantitative evaluation of tyrosine accessibility in the complex include quenching by DNA, the unknown quantum yields of individual residues, and some static quenching of tyrosine residues by acrylamide. The latter effect is evident from the upward deviation from linearity of Figure 7A.

In contrast, tryptophan fluorescence quenching differs between the free and DNA-bound protein (Figure 7B, Table 2). Values of K_{sv} for tryptophan are comparable among TBP monomers and octamers and the model protein HSA and much lower than that of N-Trp. The conclusion drawn from these results is that the tryptophan is buried in unliganded TBP. Upon formation of a complex with DNA, K_{sv} doubles compared with the free protein (Figure 7B; Table 2). This effect can be only partly explained by the increased quantum yield of tryptophan fluorescence in the complex. The increased accessibility of tryptophan along with the red shift of the fluorescence spectrum suggests that the region of the N-terminal domain of TBP containing this residue unfolds within the TBP−DNA complex.

The preliminary conclusion drawn from the anisotropy studies, presented above, was that the mobility of the

Table 2: Acrylamide Quenching of TBP Tyrosine and Tryptophan Fluorescence

sample	tyrosine fluorescence		
	A^b	A_0	K_{sv} (M^{-1})^c
1 μM TBP	0.155	0.189 ± 0.026	12.1 ± 0.6
6 μM TBP	0.160	0.196 ± 0.002	11.9 ± 0.7
TBP + DNA^a	0.157	0.213 ± 0.002	9.8 ± 0.2
1 μM HSA	0.167	0.189 ± 0.001	10.0 ± 0.2
N-Tyr	0.01	−	38.0 ± 1.6

sample	tryptophan fluorescence			
	A^b	A_0	K_{sv} (M^{-1})^c	Θ_{rel}(Trp)^d
1 μM TBP (monomeric)	0.103	0.212 ± 0.030	6.9 ± 0.2	−
6 μM TBP (octameric)	0.112	0.238 ± 0.008	6.8 ± 0.2	1.13
TBP + DNA^a	0.076	0.152 ± 0.003	13.4 ± 0.2	1.8
1μM HSA	0.146	0.169 ± 0.004	7.5 ± 0.1	−
N-Trp	0.008	−	20.4 ± 1.4	−

^{a} TBP+DNA = 6 μM TBP + 7 μM DNA. ^{b} The estimated error in the values of A was less than 1% in all cases except for N-Tyr and N-Trp, for which it was ∼10%. ^{c} K_{sv} (M^{-1}) is the Stern−Volmer constant (eq 3). ^{d} Θ_{rel}(Trp) is the relative change in the correlation time of the tryptophan residue between TBP monomers and octamers or between TBP free and bound to DNA (calculated using eq 5).

C-terminal domain is invariant upon DNA binding while the mobility of the N-terminal domain of TBP increases. However, anisotropy depends not only on the fluorescence correlation time but also on the fluorescence lifetime and the limiting value of the anisotropy. The change in the correlation time of the chromophore following the quenching of tyrosine or tryptophan fluorescence was measured using eqs 4 and 5 (Figure 8). The limiting values of the anisotropy (A_0), derived from the intersection points of the graphs with the vertical axis, are different for tyrosine and tryptophan fluorescence (Table 2).

The anisotropy, A, determined for the tyrosine fluorescence of TBP is high, close to its limiting value, A_0, and comparable with the model protein HSA. Since the quantum yield of tyrosine fluorescence is the same in TBP monomers and octamers (Table 1), the correlation time of the C-terminal domain of TBP is unchanged (eq 4) despite the 8-fold increase in molecular weight. Ligation with DNA results in a small increase in A_0, consistent with restriction of internal motions of tyrosine residues (Table 2). While the large decrease in the quantum yield of tyrosine fluorescence of TBP upon DNA binding (Figure 3) makes comparison of the correlation times difficult, high anisotropy values close to the limiting value argue for the tyrosine residues within the C-terminal domain being almost motionless.

The anisotropy of tryptophan fluorescence of free TBP is much lower than A_0 (Figure 8B; Table 2), consistent with high mobility of the residue within TBP. This result contrasts with the high tryptophan anisotropy determined for HSA that is close to its value of A_0 (Table 2). The low value of A_0 for HSA is due to the high rotational freedom of its single tryptophan (*37*). DNA binding by TBP results in a significant decrease in both A and A_0 for tryptophan (Figure 8B; Table 2). The relative change in the correlation time of tryptophan between TBP monomers and octamers is small [Θ_{rel}(Trp); Table 2], reflecting little change in the relative mobility of the N-terminal domain upon oligomerization.
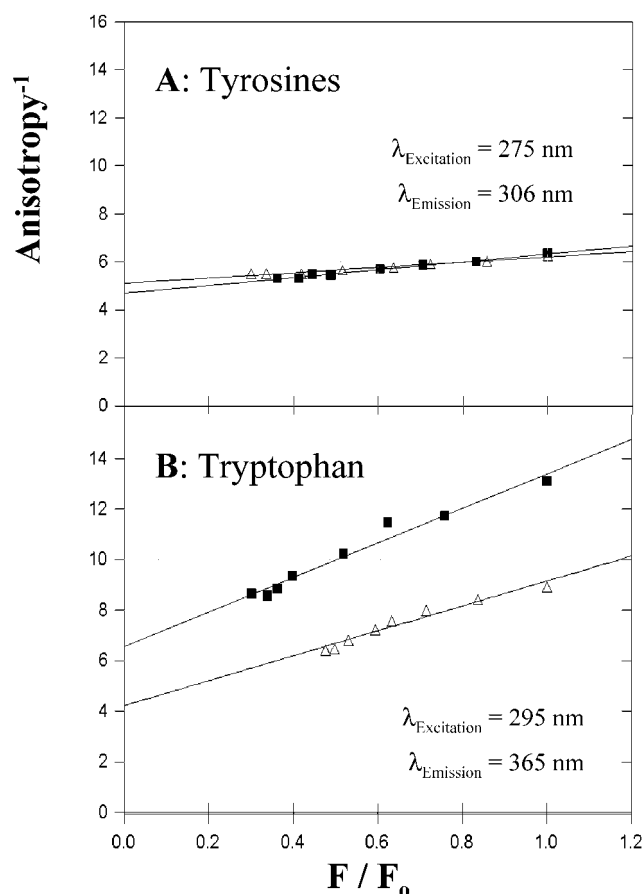
FIGURE 8: Perrin plots for the quenching resolved emission anisotropy by acrylamide of (A) tyrosine fluorescence (excitation at 275 nm and emission at 306 nm) and (B) tryptophan fluorescence (excitation at 295 nm and emission at 365 nm) for TBP at 6 μM (triangles) and for TBP at 6 μM complexed with 1.2 molar excess of DNA bearing the sequence TATAAAAG (squares).

Since the limiting anisotropy A_0 depends on both the global motion of the protein molecule and the internal rotation of the chromophore, the internal mobility of the tryptophan residue leads to fluorescence depolarization and hence to decreased A_0. Thus, the low value of A_0 of 0.152 for the TBP−DNA complex is due to increased segmental motions of the tryptophan residue. This result is consistent with the partly unfolded structure of the N-terminal domain deduced from the red-shifted λ_{max} of the fluorescence spectrum (Figure 5, Table 1) and the accessibility of tryptophan to the neutral quencher acrylamide (Figure 7, Table 2).

The large relative change in the correlation time of the N-terminal domain in the free and DNA-bound protein is a lower estimate of the domain's global motion due to the internal motions of the tryptophan residue (Table 2). The independent behavior of the N- and C-terminal domains of TBP results in a constant correlation time of the tryptophan within the N-terminal domain despite the 8-fold increase in the molecular weight upon oligomerization. Therefore, the large increase in this correlation time upon DNA binding suggests a more intimate association of the two domains in the complex. In other words, the correlation time of tryptophan reflects the mobility of the TBP−DNA complex while the mobility of only the N-terminal domain is reported for the unliganded monomeric and octameric protein.

Molecular Dynamics Simulations. The solvent accessibility of the six conserved tyrosine residues (residues 94, 139, 185,

195, 224, and 231 in yeast TBP) within the C-terminal domain was calculated from an ensemble of TBP dynamics simulations that includes three TBP monomers and six TBP−DNA complexes. Figure 9A summarizes the accessibility of these residues. They are grouped into three classes: (1) 'completely buried' with accessibility below 1% (Y139); (2) 'slightly exposed' with average accessibility <20% (Y94, Y185, and Y195); and (3) 'significantly exposed' with accessibility 20−30% (Y224 and Y231). The solvent accessibility of these residues is the same in the TBP−DNA complex, in agreement with the experimental results (Figure 7A). Measurements derived directly from the crystal coordinates of free TBP (*12*, *13*) and TBP−DNA complexes (*3*, *4*, *6−8*) yield lower solvent accessibilities although the overall trends present in the simulations are preserved. This result suggests that TBP undergoes breathing motions in solution that are not seen in the crystals due to the low temperatures used for crystallographic data collection (around 100 K).

Solvent accessibility and dynamic behavior are related. The most buried residues (Y139 and Y195) have the lowest mobility and the most exposed (Y224 and Y231) the highest (Figure 9B,C).[2] Most of the tyrosines rattle about one equilibrium position; the difference among them is the amplitude of the rattling, which can range from 90° to 180° in χ_2 (Figure 9C). As expected, the crystal structures indicate a much stiffer environment for the tyrosines than that displayed in the simulations. With regard to motion along χ_2, it is impossible to tell if a ring flip occurred in the crystal structures, as the tyrosine ring is identical in both conformations. This symmetry results in the large discrepancy in amplitude for Y224. There is no difference in the rattling amplitude upon complex formation with DNA, in agreement with the almost negligible increase in anisotropy measured experimentally (Figure 6).

The two exceptions to the low-amplitude rattling of tyrosine side chains are Y224 and Y231. The ring of Y224 flips in various simulations, corresponding to an amplitude of 360° in motion along χ_2. This motion, with a characteristic time of ∼1 ns, is predicted to lower the observed anisotropy. Either low quantum yield or the presence of the N-terminal domain in the intact protein could account for the experimentally observed high anisotropy. Y231 is the only conserved tyrosine that samples more than one χ_1 rotamer (Figure 9, with an amplitude in motion along χ_1 over 120°). This sampling is likely due to the displacement of the residues at the N-terminal end of the C-terminal domain, which cage Y231 in some of the available TBP and TBP−DNA crystal structures. This conjecture is supported by the inability of this residue to rotate in the crystal structures.

DISCUSSION

The sequence-specific binding of TBP to DNA displays unusual functional characteristics in addition to its unique structure. Its high equilibrium binding affinity masks unusually slow rates of DNA association and dissociation (*18*, *20*, *21*, *38*). Recent kinetic studies have revealed the presence

---

[2] The results presented in this paper focus upon the subject of our experimental studies. However, it is instructive to note that a nonconserved tyrosine in *A. thaliana* TBP (corresponding to F177 in yeast TBP) is characterized by solvent accessibilities that reach 90% and carries out both ring flips and sampling of more than one χ_1 rotamer.
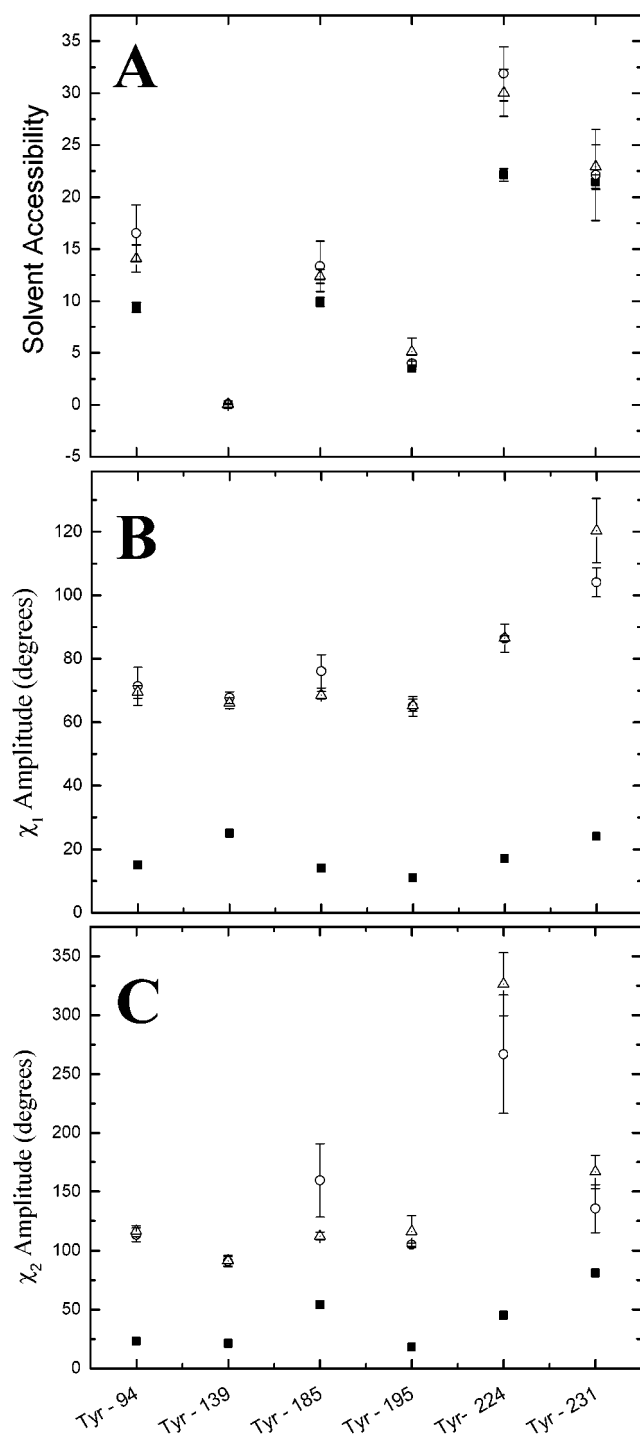
FIGURE 9: Solvent accessibility and side chain mobility of the tyrosine residues calculated from molecular dynamics simulations of the C-terminal domain of TBP. (A) Percent solvent accessibility of the six conserved tyrosine side chains of TBP relative to that of free tyrosine; (B) amplitude of motion along χ_1 for the six conserved tyrosines; and (C) amplitude of motion along χ_2 for the six conserved tyrosines. The black squares correspond to data calculated for the available crystal structures of free TBP (12, 13) and the binary TBP–DNA complexes (3, 4, 6–8), a total of 28 structures. The circles correspond to the properties calculated for the simulations of free TBP (3 simulations) and the triangles to TBP in complex with DNA (6 simulations). The error bars represent the standard error of the mean.

of two intermediates in a complex reaction pathway (22, 39). The sequence-specific binding of TBP to DNA is considered a defining example of "indirect readout" in which macro-

molecular structure and conformational accommodation are the key elements of molecular recognition. The large distortion of the DNA observed within the cocrystal structures that have been solved has suggested its conformational change as the dominant contribution to the "indirect readout" mechanism. The modest changes observed for the structure of the C-terminal domain of TBP in the crystal structures of the DNA-bound and free protein (only slight rotation of two subdomains within the C-terminal domain of TBP is observed) suggest that the protein is a passive and rigid element in the formation of the protein–DNA complex.

The present study is the first solution analysis of the structure of the C-terminal domain of TBP within the native molecule free and complexed with DNA. The basis of this analysis is the isolation of the fluorescence of the six tyrosine residues, all of which are within the C-terminal domain, and the fluorescence of the single tryptophan located within the N-terminal domain of TBP. The unusually short λ_{max} of TBP fluorescence reflects the unusually high quantum yield of the tyrosine residues within TBP. The large (36 nm) shift of the TBP fluorescence emission spectrum that results from DNA binding (Figure 5) is mainly due to quenching of tyrosine fluorescence by DNA and not to a red-shift of tryptophan fluorescence, as previously concluded (18). The values of λ_{max} (Figure 5), quantum yield (Table 1), and tyrosine fluorescence anisotropy (Figure 6) measured for the TBP–DNA complex are the same within experimental error when the TBP was monomeric or octameric prior to complex formation.

The phenomenon of fluorescence anisotropy depends on the rate at which the orientation of the excited chromophore is randomized. The randomization rate depends in turn both on the internal mobility of the chromophore within the macromolecule and on the mobility of the protein molecule as the whole. That the C-terminal domain of TBP has the same compact rigid structure in monomers, octamers, and complexed with DNA is shown from its invariant tyrosine fluorescence anisotropy (Table 2). As shown in the molecular dynamics simulations, some of the phenol rings of the tyrosines are firmly anchored and motionless, while some are mobile within the isolated C-terminal domain. Hence, the high "average" value of tyrosine anisotropy of TBP reflecting their low mobility (Table 2) may be due to low fluorescence quantum yields for residues Y224 and Y231, interdomain interactions, or both factors.

Efficient energy transfer from the tyrosine residues to the base pairs of DNA occurs in the range of 15–20 Å (32, 33). The efficient quenching of the tyrosine fluorescence of TBP in the DNA complex (Figure 5) is a solution demonstration of the intimate association of the 'saddle' of TBP with DNA along its entire length as observed in TBP–DNA cocrystal structures (3–8). This result was obtained with a high-affinity and transcriptionally-efficient TATA box sequence.

The end-to-end distances and distance distributions of complexes of TBP with oligonucleotides bearing variant TATA sequences determined by time-resolved FRET between a fluorescence donor and acceptor attached to opposite ends of the DNA differ significantly (9). At the same time, the conformation of some variant sequences is highly dependent upon the presence of osmolyte (10). A possible mechanism underlying the more dynamic behavior of the
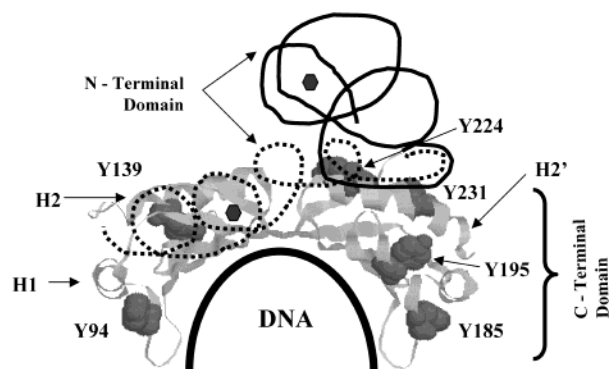
FIGURE 10: Model for the relationship between the N- and C-terminal domains of *S. cerevisiae* TBP molecule free and bound to DNA. The positions of the six conserved tyrosines in the C-terminal domain are highlighted, as is the single tryptophan (W26) of the N-terminal domain. The conformation of the N-terminal domain in free TBP is denoted by the solid line while its conformation in the TBP−DNA complex is denoted by the dashed line. Helices H1, H2, and H2′ are as designated in (*4, 11*).

TBP−variant TATA complexes observed by FRET is that contacts between the protein and DNA along the interface are not uniformly close (*9*). If so, decreased tyrosine quenching by the bound DNA might be expected for complexes with the variant sequences demonstrating increased end-to-end distances and distance distributions.

The molecular dynamics simulations were conducted in order to provide structural insight into the high fluorescence anisotropy and low accessibility of the tyrosine residues for the external quencher, within the conserved C-terminal domain seen in the present experimental studies of the full-length *S. cerevisiae* TBP. The tyrosines behave in practically the same fashion in all the simulations conducted for C-terminal domains from plant, yeast, and human sources, both free and in complexes with TATA boxes of high and medium affinity. This feature allows for averaging over all the structures and improving the quality of the conclusions that can be reached from the simulations.

The similarity in dynamics and accessibility across species is due to the high conservation of the tyrosines and their immediate neighbors.[3] Most of the tyrosines in TBP are caged by hydrophobic side chains that hinder their motions, thus accounting for both their high and invariant anisotropy and their insensitivity to quencher. For example, Y139 lies in a hydrophobic pocket and engages in strong hydrogen bonds to both the side chain and the main chain of threonine 111, another conserved residue across the three studied species. The exception is Y224, which lies on the solvent-exposed face of helix 2′ and is flanked by R220 on one side. This arginine side chain samples various rotamers (an average of nine) during the simulations and possibly causes the only ring flip observed for a tyrosine side chain in TBP. It should be noted that Y224 and Y231 are the tyrosine residues most likely to be affected by the presence of the N-terminal domain (Figure 10, discussed further below).

Unlike the C-terminal domain of TBP for which extensive atomic resolution structural information is available, little is known about the structure of the nonconserved N-terminal domain and possible interdomain interactions. The noncon-

served N-terminal domain of *S. cerevisiae* TBP (whose structure has not been solved crystallographically) has been shown by solution methods to have a flexible conformation and to be sensitive to protein self-association (*18, 19*). Biochemical studies indicate a role for the N-terminal domain of human TBP in RNA polymerase III-specific preinitiation complex formation (*40*). Genetic studies indicate multiple functions for the N-terminal domain of *S. cerevisiae* TBP (*41*). The N-terminal domains of human (*40*) and yeast TBP (*42, 43*) have been reported to destabilize the complex with DNA. The approach developed herein permits the separation of the tryptophan and tyrosine fluorescence of TBP to provide new insight into the structure of the N-terminal domain of TBP and its relationship with the C-terminal domain.

The TBP octamer is a 'loose' structure in which the N- and C-terminal domains of each monomer behave independently [(*17, 19*) and herein]. Dramatic changes in the structure of the N-terminal domain are evident when TBP binds to DNA. That the N-terminal domain unfolds upon formation of the TBP−DNA complex is inferred from several lines of evidence. This evidence includes the long-wavelength shift of the fluorescence spectrum (Figure 5, Table 1), the doubling of the Stern−Volmer constant, K_{sv}, for tryptophan (Table 2), and the decrease in the limiting value of the tryptophan anisotropy (Figure 6, Table 2).

The decrease in the anisotropy of tryptophan fluorescence of TBP upon binding to DNA (Figure 6, Table 2) is not proof of increased N-terminal domain mobility as previously concluded (*18*). To the contrary, the correlation time of the N-terminal domain almost doubles upon DNA complex formation (Table 2). The results of studies conducted using the quenching resolved emission anisotropy method (*24*) show that the majority of the tryptophan fluorescence anisotropy decrease is due to a decrease in the limiting anisotropy, A_0 (Table 2). Since the anisotropy A depends on both the global motion of the protein molecule and the internal rotation of the chromophore, the decrease of the limiting anisotropy A_0 is due to an increase in the internal depolarizing motion of the tryptophan residue in the protein−DNA complex. The increased rotational freedom of the tryptophan residue is consistent with other changes in the tryptophan fluorescence (Table 2). These results infer that despite 'unfolding' of the N-terminal domain, it more intimately associates with the C-terminal domain in the TBP−DNA complex.

The characterization of the structural transition of the N-terminal domain upon binding to DNA provides new insight into the structure−function relationships of the two domains of TBP. Conformational freedom makes it possible for TBP to achieve suitable binding contacts with DNA moieties in a dynamic mode (*44*). In addition, structural changes in the N-terminal domain in the protein−DNA complex may provide an additional allosteric mechanism that enhances sequence-specific binding of DNA as well as subsequent interaction with RNA polymerase general transcription factors.

A general scheme that summarizes the consistencies and changes in the structure of yeast TBP that occur upon DNA binding is shown in Figure 10. TBP interacts with DNA as a monomer. The C-terminal domain has the compact rigid structure that is invariant with most of the phenol rings of its tyrosines firmly anchored and relatively motionless

---

[3] The six tyrosines present in yeast TBP are also in human and plant TBP. Plant TBP has one extra tyrosine.

(Figure 9). These conclusions are based upon the low accessibility of the tyrosines to external quencher and that the fluorescence anisotropy is close to its limiting value. The C-terminal domain is uniformly close enough to the DNA so that effective fluorescence quenching of all the tyrosines by DNA base pairs occurs in the TBP−DNA complex.

In contrast, the structure of the N-terminal domain changes upon DNA binding by TBP. That the N-terminal domain neither contacts nor is in proximity to the bound DNA (Figure 10, solid line conformation) is shown by the absence of tryptophan fluorescence quenching in the TBP−DNA complex. The fluorescence red-shift of the tryptophan reporting of a more polar environment in the complex, the high accessibility of the tryptophan residue to external quencher, and its increasing internal motion within the N-terminal domain indicate that the N-terminal domain unfolds in the TBP−DNA complex. However, despite the unfolded structure, the correlation time of the N-terminal domain increases, showing its reduced flexibility in the complex with DNA (Figure 10, dashed line conformation). These conformational changes may influence the further subsequent events in formation of the transcription preinitiation complex.

Tyrosines 224 and 231 are the most exposed tyrosine residues and are located within the last alpha helix (H2′) of the C-terminal domain, facing outward in the isolated C-terminal domain structures (Figure 10); helix 2′ contacts also the first seven residues of the C-terminal domain of TBP. These tyrosines are also the most mobile in the molecular dynamics simulations of the isolated domain (Figure 9). It is likely that Y224 and Y231 are sensitive to the presence of the N-terminal domain present in the full-length protein. Hypothetically, wrapping of the N-terminal domain over helix 2′ would wedge Y224 between V64 and R220 and bury Y231 by I62, P132, and S235 (Figure 10). Is there evidence to support this conjecture?

The low unchanged fluorescence anisotropy (Figure 6, Table 2) and unchanged mobility of Y224 and Y231 in the TBP−DNA complex as compared with free TBP (Figure 9) argue that only some portions of the N-terminal domain change position relative to the C-terminal domain upon TBP−DNA complex formation. The most likely candidate for invariant interactions with the C-terminal domain is the N-terminal polypeptide closest to the C-terminal core. This conjecture is consistent with genetic studies (*41*) demonstrating that the final 10 residues of the N-terminal domain (that we propose to wrap over helix 2′) are required for the viability of cells bearing TBP mutants that are lethal in the context of the isolated C-terminal core domain.

Protein "footprinting" data indicate DNA binding modulated interactions of the N-terminal domain of TBP with the C-terminal domain such as shown in Figure 10 that are consistent with the fluorescence changes observed in the present study (H. Rashidzadeh, S. Khrapunov, M. R. Chance, and M. Brenowitz, manuscript in preparation). As is suggested in Figure 10, only the initial residues of the N-terminal domain (including W26) unfold and extend in the direction of the H2 and H1 helices of the C-terminal domain. While the precise interactions between the N- and C-terminal domains of *S. cerevisiae* TBP remain to be determined, the present fluorescence studies have clearly defined the nature of the DNA ligation dependent changes that occur.

REFERENCES

1. Lee, D. K., Wang, K. C., and Roeder, R. G. (1997) *Nucleic Acids Res. 25*, 4338−4345.
2. Reese, J. C., Zhang, Z., and Kurpad, H. (2000) *J. Biol. Chem. 275*, 17391−17398.
3. Kim, J. L., Nikolov, D. B., and Burley, S. K. (1993) *Nature 365*, 520−527.
4. Kim, Y., Geiger, J. H., Hahn, S., and Sigler, P. B. (1993) *Nature 365*, 512−520.
5. Kim, J. L., and Burley, S. K. (1994) *Nat. Struct. Biol. 1*, 638−653.
6. Juo, Z. S., Chiu, T. K., Leiberman, P. M., Baikalov, I., Berk, A. J., and Dickerson, R. E. (1996) *J. Mol. Biol. 261*, 239−254.
7. Nikolov, D. B., Chen, H., Halay, E. D., Hoffman, A., Roeder, R. G., and Burley, S. K. (1996) *Proc. Natl. Acad. Sci. U.S.A. 93*, 4862−4867.
8. Patikoglou, G. A., Kim, J. L., Sun, L., Yang, S. H., Kodadek, T., and Burley, S. K. (1999) *Genes Dev. 13*, 3217−3230.
9. Wu, J., Parkhurst, K. M., Powell, R. M., Brenowitz, M., and Parkhurst, L. J. (2001) *J. Biol. Chem. 276*, 14614−14622.
10. Wu, J., Parkhurst, K. M., Powell, R. M., and Parkhurst, L. J. (2001) *J. Biol. Chem. 276*, 14623−14627.
11. Nikolov, D. B., Hu, S. H., Lin, J., Gasch, A., Hoffmann, A., Horikoshi, M., Chua, N. H., Roeder, R. G., and Burley, S. K. (1992) *Nature 360*, 40−46.
12. Chasman, D. I., Flaherty, K. M., Sharp, P. A., and Kornberg, R. D. (1993) *Proc. Natl. Acad. Sci. U.S.A. 90*, 8174−8178.
13. Nikolov, D. B., and Burley, S. K. (1994) *Nat. Struct. Biol. 1*, 621−637.
14. DeDecker, B. S., O'Brien, R., Fleming, P. J., Geiger, J. H., Jackson, S. P., and Sigler, P. B. (1996) *J. Mol. Biol. 264*, 1072−1084.
15. Longworth, J. W. (1983) in *Time-resolved Fluorescence Spectroscopy in Biochemistry and Biology* (Cundall, R. B., and Dale, R. E., Eds.) pp 651−686, Plenum Press, New York and London.
16. Lakowicz, J. R. (1999) *Principles of Fluorescence spectroscopy*, 2nd ed., Kluwer Academic/Plenum, New York.
17. Daugherty, M. A., Brenowitz, M., and Fried, M. G. (1999) *J. Mol. Biol. 285*, 1389−1399.
18. Perez-Howard, G. M., Weil, P. A., and Beechem, J. M. (1995) *Biochemistry 34*, 8005−8017.
19. Daugherty, M. A., Brenowitz, M., and Fried, M. G. (2000) *Biochemistry 39*, 4869−4880.
20. Petri, V., Hsieh, M., and Brenowitz, M. (1995) *Biochemistry 34*, 9977−9984.
21. Parkhurst, K. M., Brenowitz, M., and Parkhurst, L. J. (1996) *Biochemistry 35*, 7459−7465.
22. Parkhurst, K. M., Richards, R. M., Brenowitz, M., and Parkhurst, L. J. (1999) *J. Mol. Biol. 289*, 1327−1341.
23. Eftink, M. R., and Ghiron, C. A. (1981) *Anal. Biochem. 114*, 199−227.
24. Eftink, M. (1983) *Biophys. J. 43*, 323−334.
25. Pastor, N., Weinstein, H., Jamison, E., and Brenowitz, M. (2000) *J. Mol. Biol. 304*, 55−68.
26. MacKerell, A. D., Jr., Bashford, D., Bellott, M., Dunbrack, R. L., Jr., Evanseck, J. D., Field, M. J., Fischer, S., Gao, J., Guo, H., Ha, S., Joseph-McCarthy, D., Kuchnir, L., Kuczera, K., Lau, F. T. K., Mattos, C., Michnick, S., Ngo, T., Nguyen, D. T., Prodhom, B., Reiher, W. E., III, Roux, B., Schlenkrich, M., Smith, J. C., Stote, R., Straub, J., Watanabe, M., Wiorkiewicz-Kuczera, J., Yin, D., and Karplus, M. (1998) *J. Phys. Chem. B 102*, 3586−3616.
27. MacKerell, A. D., Jr., Wiorkiewicz-Kuczera, J., and Karplus, M. (1995) *J. Am. Chem. Soc. 117*, 11946−11975.
28. Sklenar, H., Etchebest, C., and Lavery, R. (1989) *Proteins: Struct., Funct., Genet. 6*, 46−60.

29. Swaminathan, S., Ravishanker, G., Beveridge, D. L., Lavery, R., Etchebest, C., and Sklenar, H. (1990) *Proteins: Struct., Funct., Genet. 8*, 179−193.

30. Brooks, B. R., Bruccoleri, R. E., Olafson, B. D., States, D. J., Swaminathan, S., and Karplus, M. (1983) *J. Comput. Chem. 4*, 187−217.

31. Khrapunov, S. N., Dragan, A. I., Sivolob, A. V., and Zagariya, A. M. (1997) *Biochim. Biophys. Acta 1351*, 213−222.

32. Helene, C., and Lancelot, G. (1982) *Prog. Biophys. Mol. Biol. 39*, 1−68.

33. Montenay-Garestier, T. (1975) *Photochem. Photobiol. 22*, 3−6.

34. Valleur, B., and Weber, G. (1977) *Photochem. Photobiol. 25*, 441−444.

35. Ghiron, C. A., and Longworth, J. W. (1979) *Biochemistry 18*, 3828−3832.

36. Turoverov, K. K., Kuznetsova, I. M., and Zaitsev, V. N. (1985) *Biophys. Chem. 23*, 79−89.

37. Munro, I., Pecht, I., and Stryer, L. (1979) *Proc. Natl. Acad. Sci. U.S.A. 76*, 56−60.

38. Hoopes, B. C., LeBlanc, J. F., and Hawley, D. K. (1992) *J. Biol. Chem. 267*, 11539−11547.

39. Powell, R. M., Parkhurst, K. M., Brenowitz, M., and Parkhurst, L. J. (2001) *J. Biol. Chem. 276*, 29782−29791.

40. Mittal, V., and Hernandez, N. (1997) *Science 275*, 1136−1140.

41. Lee, M., and Struhl, K. (2001) *Genetics 158*, 87−93.

42. Kuddus, R., and Schmidt, M. C. (1993) *Nucleic Acids Res. 21*, 1789−1796.

43. Horikoshi, M., Yamamoto, T., Ohkuma, Y., Weil, P. A., and Roeder, R. G. (1990) *Cell 61*, 1171−1178.

44. Pastor, N., and Weinstein, H. (2000) in *Theoretical Biochemistry: Processes and Properties of Biological Systems* (Eriksson, L. A., Ed.) Elsievier Science, New York.